



Planarized B,N-Phenylated Dibenzazaborine with a Carbazole Substructure: Electronic Impact of the Structural Constraint

Journal:	<i>Organic & Biomolecular Chemistry</i>
Manuscript ID	OB-COM-04-2019-000934.R1
Article Type:	Communication
Date Submitted by the Author:	14-May-2019
Complete List of Authors:	Ando, Mikinori; Nagoya University, Department of Chemistry, Graduate School of Science Sakai, Mika; Nagoya University, Department of Chemistry, Graduate School of Science Ando, Naoki; Nagoya University, Department of Chemistry, Graduate School of Science Hirai, Masato; Nagoya University, Department of Chemistry, Graduate School of Science Yamaguchi, Shigehiro; Nagoya University, Department of Chemistry, Graduate School of Science

COMMUNICATION

Planarized *B,N*-Phenylated Dibenzazaborine with a Carbazole Substructure: Electronic Impact of the Structural Constraint

Received 00th January 20xx,
Accepted 00th January 20xx

Mikinori Ando,^a Mika Sakai,^a Naoki Ando,^a Masato Hirai,^b and Shigehiro Yamaguchi^{*a,b}

DOI: 10.1039/x0xx00000x

A *B,N*-diphenyl-5,10-dihydro-dibenzo-1,4-azaborine, in which both phenyl groups on the boron and nitrogen atoms are planarized to generate a carbazole substructure, was synthesized. The structural constraint around the boron and nitrogen atoms alters the π -conjugation mode and thus the photophysical and electrochemical properties. Specifically, this structurally constrained dibenzazaborine showed an intense blue emission with a narrow full width at half maximum. One of its derivatives exhibited near infrared absorption in the one-electron-oxidized state.

Embedding heteroatoms into polycyclic aromatic hydrocarbons (PAHs) is an effective way to alter their structural and electronic properties by capitalizing on the size effects, the inductive effects, and the orbital interactions of the heteroatoms.¹ Based on this design strategy, a variety of fascinating π -electron materials have been synthesized.² PAHs containing multiple heteroatoms are particularly important as synergistic effects of the heteroatoms can give rise to intriguing electronic properties. For example, *B,N*-containing PAHs have attracted significant attention as the boron and nitrogen atoms have complementary electron-accepting and -donating properties.³

One way of embedding boron and nitrogen atoms is to use *B-N* bonds as an isostere of the $C=C$ double bond, and several PAHs containing *B-N* bonds have been developed and used in organic electronic devices including organic field-effect transistors (OFETs).⁴ Another strategy is to embed boron and nitrogen atoms in remote positions with respect to each other, as exemplified by a *B,N*-diphenyl-5,10-dihydro-dibenzo-1,4-azaborine **A** (hereafter abbreviated as dibenzazaborine) (Figure 1a). Kawashima and co-workers have synthesized a series of

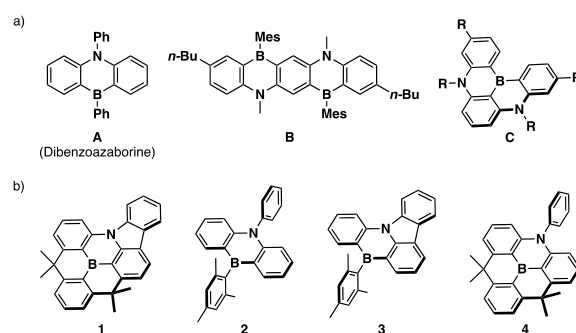


Figure 1. (a) Representative examples of previously reported dibenzazaborine-based π -conjugated compounds and (b) planarized *B,N*-phenylated dibenzazaborine **1** together with reference compounds **2–4**.

acene-like π -extended dibenzazaborines such as compound **B** that show intriguing photophysical properties.⁵ Recently, Hatakeyama and co-workers have synthesized a series of PAHs that contain multiple 1,4-azaborine rings, and some of these PAHs represented by compound **C** showed excellent thermally activated delayed fluorescence (TADF) with pure-blue colors of a narrow full width at half maximum (FWHM). Some of these PAHs have subsequently been employed in organic light-emitting diodes (OLEDs).⁶

The aforementioned results demonstrate the promising potential of the dibenzazaborine skeleton as a building block for π -electron materials. However, further advancements in this class of materials should require a more detailed understanding of the relationship between their structure and their electronic structure, and hence their photophysical and electrochemical properties. In this context, we are interested in the correlation between the ring-fusion mode and the degree of structural constraint within the dibenzazaborine skeleton. The structural constraint into a planar fashion is an effective strategy to expand the π -conjugation and to increase the chemical stability.^{2c} We have already demonstrated that the fixation of three aryl groups of triarylboranes into a planar structure effectively stabilizes such compounds, even in the absence of steric protection on the boron center.⁷ On the other hand,

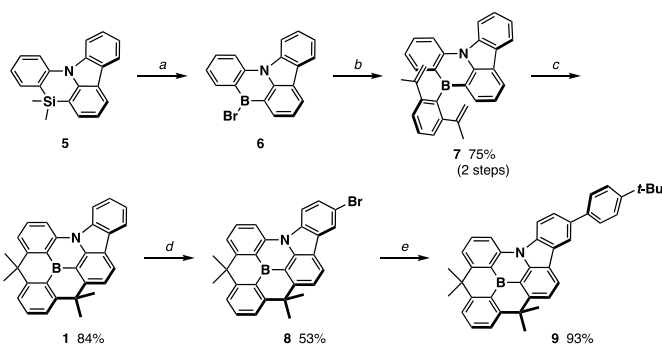
^a Department of Chemistry, Graduate School of Science, Nagoya University, Furo, Chikusa, Nagoya, 464-8602, Japan.

^b Integrated Research Consortium on Chemical Sciences (IRCCS), Nagoya University, Furo, Chikusa, Nagoya, 464-8602, Japan. Institute of Transformative Bio-Molecules (WPI-ITbM), Nagoya University, Furo, Chikusa, Nagoya, 464-8602, Japan. E-mail: yamaguchi@chem.nagoya-u.ac.jp.

*Electronic Supplementary Information (ESI) available: Experimental procedures, spectral data, details of the computational studies, and crystallographic data for **1** and **4**. CCDC 1911122–1911123. See DOI: 10.1039/x0xx00000x

planarization of the triphenylamine skeleton to form a carbazole substructure decreases the electron-donating ability of the amine moiety.⁸ These considerations encouraged us to modify the *B*- and *N*-phenyl groups in the dibenzoazaborine in a planar fashion to generate a new family of planarized triarylboranes with a carbazole substructure (**1**; Figure 1b). To better understand the impact of the structural constraint on the electronic structure and the photophysical and electrochemical properties of **1**, compounds **2–4** were synthesized as reference compounds for comparison.

Compound **1** was prepared in three steps from silicon-bridged *N*-phenylcarbazole **5** (Scheme 1). The silicon-boron exchange reaction of **5** with BBr₃ proceeded smoothly and a subsequent treatment of **6** with 2,6-di(propen-2-yl)phenyllithium provided **7** in 75% yield. Two-fold intramolecular Friedel–Crafts cyclization of **7** in the presence of Sc(OTf)₃ furnished **1** in 84% yield.^{7a} Compound **1** was sufficiently stable to be purified by standard column chromatography on silica gel. Moreover, the boron moiety in **1** showed desirable robustness against electrophiles and nucleophiles, which allowed further functionalization of the carbazole moiety in **1** by conventional methods. Specifically, the bromination of **1** with *N*-bromosuccinimide occurred at the benzene ring of the carbazole moiety to furnish bromo-substituted **8**. Subsequent cross-coupling reactions of **8** successfully afforded the corresponding π -expanded derivatives. For instance, the Suzuki–Miyaura coupling of **8** with 4-*t*-butylphenylboronic acid under basic conditions produced **9** in 93% yield. For comparison, **3** was synthesized by a procedure similar to that of **1**, while **2** and **4** were prepared *via* literature procedures (Schemes S1 and S2).^{5a}



Scheme 1 Synthesis of **1** and π -expanded derivative **9**. *Reagents and conditions:* (a) BBr₃, CH₂Cl₂, r.t.; (b) 2,6-di(propen-2-yl)phenyllithium, toluene, 50 °C; (c) Sc(OTf)₃, 1,2-dichloroethane, 60 °C; (d) NBS, CH₂Cl₂, r.t.; (e) 4-*t*-butylphenylboronic acid, Pd(PPh₃)₄, K₂CO₃, toluene/H₂O, reflux.

The solid-state structure of **1** was determined unambiguously by a single-crystal X-ray diffraction analysis (Figure 2), which revealed a highly planar structure for **1**, albeit that the *N*-phenylcarbazole substructure is slightly distorted due to the steric repulsion between the carbazole moiety and the *N*-phenyl group. Both the boron and nitrogen atoms adopt a trigonal planar geometry with bond-angle sums of 359.9° around the B1 and N1 atoms, indicative of effective π -interaction around the boron and nitrogen centers. The B–C

bond lengths [B1–C1: 1.512(2) Å; B1–C17: 1.493(2) Å; B1–C19: 1.507(2) Å] are shorter than those of a previously reported dibenzoazaborine derivative with a mesityl group on the boron atom [B–C: 1.522(3)–1.584(3) Å].⁹ This difference should be attributed to the planarization of the *B*-phenyl group, as **4** also exhibits B–C bond lengths that are comparable to those of **1** (Figure S2 and Table S1). The contracted B–C bonds, resulting from the structural constraint around the boron atom, imply that effective electron donation occurs from the benzene rings to a vacant p orbital of the boron atom,^{7a,10} which probably contributes to the high chemical stability of **1**.

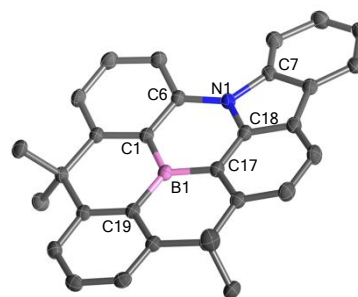


Figure 2. Crystal structure of **1** (thermal ellipsoids at 50% probability; hydrogen atoms are omitted for clarity). Selected bond lengths (Å) and angles (°): B1–C1 = 1.512(2), B1–C17 = 1.493(2), B1–C19 = 1.507(2), C1–B1–C17 = 118.0(1), C1–B1–C19 = 122.9(1), C17–B1–C19 = 119.0(1), C6–N1–C7 = 131.6(1), C6–N1–C18 = 121.7(1), C7–N1–C18 = 106.6(1).

Subsequently, we carried out a comparison of the photophysical properties of **1** and **2–4** (Figure 3 and Table 1). The UV-vis absorption spectrum of **2** in THF exhibited absorption band maxima (λ_{abs}) at 389 and 371 nm, while that of *N*-phenyl-fused **3** showed one maximum at $\lambda_{\text{abs}} = 400$ nm. Comparable λ_{abs} values were also observed in the *B*-phenyl-planarized derivatives, *i.e.*, **4** showed absorption bands with a vibronic structure at $\lambda_{\text{abs}} = 404$ and $\lambda_{\text{abs}} = 387$ nm, while *N*-phenyl-fused **1** exhibited an intense absorption band at $\lambda_{\text{abs}} = 402$ nm.

The fluorescence spectra of **1–4** in THF exhibited an intense blue emission with a narrow FWHM. Specifically, **1** showed an intense deep blue emission ($\lambda_{\text{em}} = 416$ nm; $\Phi_{\text{F}} = 0.82$) with a FWHM of 27 nm, which is most likely due to the rigid structure of **1** that leads to a loss of the vibronic structure.

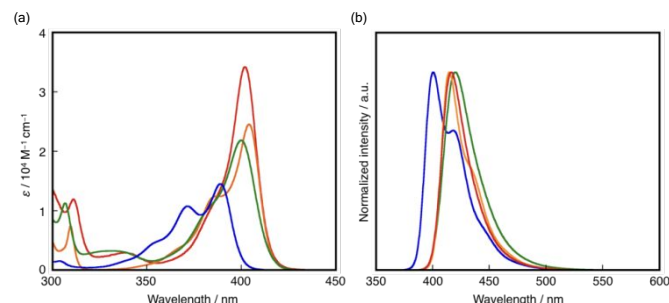


Figure 3. (a) UV-vis absorption and (b) fluorescence spectra of **1** (red), **2** (blue), **3** (green) and **4** (orange) in THF.

To understand the effects of the structural constraint on the electronic properties, DFT calculations were carried out for **1–4**

at the B3LYP/6-31G(d) level of theory (Figure 4). The optimized structure for **1** at this level of theory is consistent with the experimentally determined crystal structure. In **2** and **4**, in which the *N*-phenyl groups are orthogonally aligned, both the highest occupied molecular orbitals (HOMOs) and the lowest unoccupied molecular orbitals (LUMOs) are delocalized over the dibenzoazaborine framework. In contrast, the HOMOs of *N*-phenyl-fused dibenzoazaborines **1** and **3** are delocalized over both the dibenzoazaborine and the carbazole moieties, while the LUMOs contain a large contribution from the boron atom. These results indicate that the structural constraint significantly affects the π -conjugation mode of the dibenzoazaborine framework.

A close inspection of the energy levels of the HOMO and LUMO provides an in-depth understanding on the impact of the structural constraint on the electronic structure. Upon planarization of the *B*-phenyl group with two methylene tethers (**2** \rightarrow **4**), the energy level of the HOMO increases, mainly due to the electron-donating effect of the alkyl groups, whereas the LUMO level remains unchanged (Figure S9).¹¹ In contrast, the fusion of the *N*-phenyl group (**4** \rightarrow **1**) decreases the HOMO and LUMO levels. To obtain further insight into the effect of the ring-fusion, we also used model compound **4'**, which has a coplanar alignment of the *N*-phenyl group relative to the dibenzoazaborine framework, for a theoretical comparison.¹² Upon changing the alignment of the *N*-phenyl group from an orthogonal to a coplanar conformation (**4** \rightarrow **4'**), the energy levels of the HOMO and LUMO decreased by 0.16 eV and 0.26 eV, respectively. These energy levels further decreased by ca. 0.1 eV upon formation of the carbazole substructure in **1**. Overall, in planarized *B,N*-phenylated **1**, the energy level of the LUMO is lower than that of **2**, while the energy level of the HOMO is comparable. These electronic effects are responsible for the red-shifted absorption of **1** compared to that of **2**.

Time dependent (TD)-DFT calculations at the same level of theory showed that the oscillator strength (*f*) also increases upon restraining the substituents on the boron and nitrogen atoms, resulting in the largest molar absorption coefficient (ϵ) value for **1** among all the relevant compounds. Thus, the planarization and the ring-fusion induces a red-shifted absorption and an increased ϵ value.

The effect of the structural constraint on the aromaticity was assessed by carrying out nucleus-independent chemical shifts (NICS) calculations at the B3LYP/6-31G(d) level of theory.¹³ The NICS(1) values for the optimized structures of **1–4** are illustrated

in Figure S5. In general, the BNC₄ ring of the dibenzoazaborine exhibits weak aromatic character as exemplified by the NICS(1) value of the BNC₄ ring in **2** (−4.4 ppm). In contrast, the BNC₄ ring in **1** exhibits a nonaromatic character with a positively shifted NICS(1) value (−1.8 ppm). In contrast, the NC₄ ring in **1** exhibits a relatively negative NICS(1) value (−6.5 ppm), indicative of maintaining an aromatic character on the NC₄ ring. These results suggest that **1** contains a more dominant contribution from the *N*-phenylcarbazole substructure rather than the azaborine substructure.

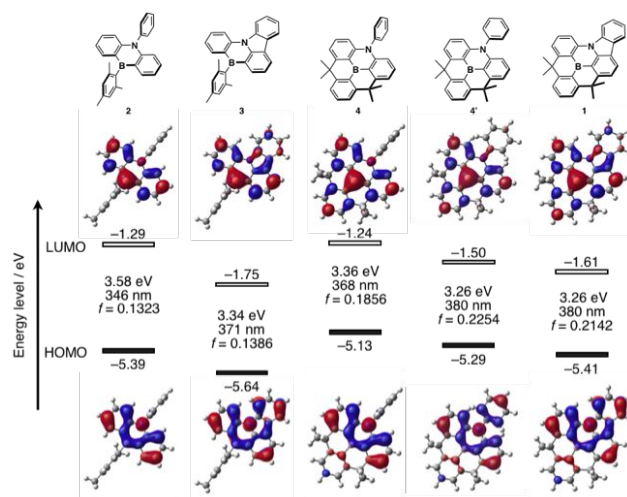


Figure 4. Energy diagram and Kohn–Sham HOMOs and LUMOs for **1–4** together with those for model compound **4'**, calculated at the B3LYP/6-31G(d) level of theory. The results of TD-DFT calculations are also shown.

The electrochemical properties of **1–4** were examined by cyclic voltammetry (CV) to experimentally confirm the electronic features imposed by the structural constraint (Figure S3 and Table 1). The cyclic voltammograms of **1–4** in THF revealed one reversible reduction wave irrespective of the structural constraint around the boron and nitrogen atoms. The half reduction potentials are positively shifted in the order **2** (−2.79 V) \approx **4** (−2.75 V) < **1** (−2.47 V) \approx **3** (−2.41 V) (vs Fc/Fc⁺), demonstrating an impact of the formation of the carbazole substructure on the energy level of the LUMOs.

The oxidation processes, which were measured in CH₂Cl₂, revealed a reversible oxidation wave for **4** with a half oxidation potential of +0.73 V (vs Fc/Fc⁺), whereas irreversible oxidation waves were observed for **1–3**. This difference is probably due to

Table 1 Photophysical and Electrochemical Properties of **1–4**

Compd	Absorption ^a		Fluorescence ^a			Oxidation potential ^{d,e}		Reduction potential ^{a,d}
	λ_{abs} [nm]	ϵ [10 ⁴ M ⁻¹ cm ⁻¹]	λ_{em} [nm]	Φ_{f} ^b	FWHM ^c [nm]	E_{pa}^{f} [V]	$E_{1/2}$ [V]	$E_{1/2}$ [V]
1	402	3.42	416	0.82	27	+1.06	–	–2.47
2	389	1.45	400	0.96	36	+1.22	–	–2.79
3	400	2.19	420	0.72	32	+1.02	–	–2.41
4	404	2.45	415	0.95	28	+0.79	+0.73	–2.75

^a In THF. ^b Absolute fluorescence quantum yields were determined by a calibrated integrating sphere system within an error of $\pm 3\%$. ^c Full width at half maximum. ^d Determined by cyclic voltammetry (supporting electrolyte: 0.1 M *n*Bu₄N⁺PF₆⁻; scan rate: 100 mV s⁻¹; internal standard: ferrocene). ^e In CH₂Cl₂. ^f Peak oxidation potential.

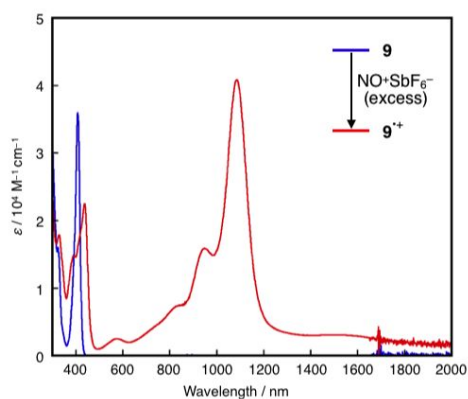


Figure 5. UV-vis-NIR absorption spectra of **9** and *in-situ*-generated radical cation **9⁺**, which was obtained *in-situ* from treatment of **9** with an excess of NO⁺SbF₆⁻ in CH₂Cl₂ (2.2 × 10⁻⁴ M).

the suppression of the dimerization of the *in-situ*-generated radical cation **4⁺** by the dimethylmethylene bridges. In general, radical cations of triphenylamine derivatives readily dimerize to form the corresponding tetraphenylbenzimidates.¹⁴ However, the *para*-position relative to the nitrogen atom in the dibenzoazaborine skeleton of **4** is likely protected by the steric hindrance of the dimethylmethylene bridges, resulting in an improved electrochemical stability of the dibenzoazaborine skeleton. In contrast, the planarization of *N*-phenyl group decreased the electrochemical stability of **1**, as the spin is delocalized onto the *N*-phenyl group. Indeed, a high spin density was theoretically confirmed at the *para*-position relative to the nitrogen atom in the carbazole substructure for the radical cation **1⁺** (Figure S7). Given this result, we assumed that in **1**, the introduction of substituents at the *para*-position relative to the nitrogen atom at the carbazole substructure could induce superior electrochemical stability. Based on this hypothesis, we synthesized 4-*t*-butylphenyl-substituted **9**, which indeed exhibited reversible redox waves with a half oxidation potential of +0.84 V (vs Fc/Fc⁺).

Encouraged by this result, the chemical oxidation of **9** was investigated by *in-situ* UV-vis-NIR absorption spectroscopy. In CH₂Cl₂, **9** showed an absorption band at $\lambda_{\text{abs}} = 408$ nm ($\epsilon = 3.60 \times 10^4$ M⁻¹cm⁻¹). Upon treatment of **9** with an excess of the oxidant NO⁺SbF₆⁻, the absorption band of **9** diminished and an intense absorption band at $\lambda_{\text{abs}} = 1085$ nm emerged

concomitant with a weak and broad absorption band at ~ 1500 nm. The new absorption band in the near-infrared (NIR) region should be attributed to radical cation **9⁺**, which is supported by the TD-DFT calculations in CH₂Cl₂ at the UB3LYP/6-31+G(d) level of theory employing a PCM model (Figure S8 and Table S3). The HOMO and SOMO are delocalized over the *t*-butylphenyl-substituted *N*-phenylcarbazole substructure with a negligible contribution from the boron atom, while the LUMO is delocalized over the *N*-phenylcarbazole moiety including the boron atom. The longest absorption band should be attributed in essence to the HOMO(β)–SOMO(β) transition, which exhibits a small oscillator strength ($f = 0.0463$) and a small transition energy (0.69 eV), consistent with the NIR absorption (1793 nm).

In summary, we have successfully synthesized a series of dibenzoazaborine derivatives **1–4**, and investigated the impact of the structural constraint on their electronic structure and hence the photophysical and electrochemical properties. A comparison of **1–4** revealed that the planarization of the *N*-phenyl group to form a carbazole substructure has a more profound effect on the electronic structure than the planarization of the *B*-phenyl group. Specifically, the planarization of the *N*-phenyl group converted the acene-like π -conjugation on the dibenzoazaborine skeleton into a boron-bridged *N*-phenylcarbazole-like π -conjugation, whereas the planarization of the *B*-phenyl group resulted mainly in an expansion of the π -conjugation. Notably, among the compounds investigated, **1** exhibited an intense blue fluorescence with a narrow full width at half maximum (27 nm). Moreover, the radical cation of π -expanded derivative **9** showed a characteristic absorption in the near infrared region. These results demonstrate the potential utility of B,N-embedded compounds in which the B and N atoms are spatially separated as building blocks for π -conjugated materials, and provide important guidelines for the molecular design of structurally constrained π -electron systems.

This work is partly supported by JSPS KAKENHI grant 18H03909 and 18H05261. M. S. thanks Graduate Program of Transformative Chem-Bio Research in Nagoya University, (MEXT, WISE program). ITbM is supported by the World Premier International Research Center (WPI) Initiative, Japan.

Conflicts of interest

There are no conflicts of interest to declare.

Notes and references

- (a) A. Fukazawa and S. Yamaguchi, *Chem. Asian. J.*, **2009**, *4*, 1386; (b) X. He and T. Baumgartner, *RSC Adv.*, **2013**, *3*, 11334; (c) S. M. Prake, M. P. Boone and E. Rivard, *Chem. Commun.*, **2016**, *52*, 9485.
- Recent reviews: (a) A. Narita, X.-Y. Wang, X. Feng, and K. Müllen, *Chem. Soc. Rev.*, **2015**, *44*, 6616; (b) M. Stępien, E. Gonka, M. Zyla and N. Sprutta, *Chem. Rev.*, **2017**, *117*, 3479; (c) M. Hirai, N. Tanaka, M. Sakai and S. Yamaguchi, *Chem. Rev.*, DOI: 10.1021/acs.chemrev.8b00637.
- For reviews on B,N-embedded PAHs, see: (a) Z. Liu and T. B. Marder, *Angew. Chem. Int. Ed.*, **2008**, *47*, 242; (b) M. J. D. Bosdet and W. E. Piers, *Can. J. Chem.*, **2009**, *87*, 29; (c) P. G. Cambell, A. J. V. Marwitz and S.-Y. Liu, *Angew. Chem. Int. Ed.*, **2012**, *51*, 6074; (d) X.-Y. Wang, J.-Y. Wang and J. Pei, *Chem. Eur. J.*, **2015**, *21*, 3528; (e) J.-Y. Wang and J. Pei, *Chin. Chem. Lett.*, **2016**, *27*, 1139; (f) J. Huang and Y. Li, *Front. Chem.*, **2018**, *6*, 341.
- (a) T. Hatakeyama, S. Hashimoto, T. Oda and M. Nakamura, *J. Am. Chem. Soc.*, **2012**, *134*, 19600; (b) X.-Y. Wang, F.-D. Zhuang, R.-B. Wang, X.-C. Wang, X.-Y. Cao, J.-Y. Wang and J. Pei, *J. Am. Chem. Soc.*, **2014**, *136*, 3764.
- (a) T. Agou, J. Kobayashi and T. Kawashima, *Org. Lett.*, **2006**, *8*, 2241; (b) T. Agou, J. Kobayashi and T. Kawashima, *Chem. Commun.*, **2007**, 3204; (c) T. Agou, H. Arai and T. Kawashima, *Chem. Lett.*, **2010**, *39*, 612.
- (a) T. Hatakeyama, K. Shiren, K. Nakajima, S. Nomura, S. Nakatsuka, K. Kinoshita, J. Ni, Y. Ono and T. Ikuta, *Adv. Mater.*, **2016**, *28*, 2781; (b) K. Matsui, S. Oda, K. Yoshiura, K. Nakajima, N. Yasuda and T. Hatakeyama, *J. Am. Chem. Soc.*, **2018**, *140*, 1195.
- (a) Z. Zhou, A. Wakamiya, T. Kushida and S. Yamaguchi, *J. Am. Chem. Soc.*, **2012**, *134*, 4529; (b) S. Saito, K. Matsuo and S. Yamaguchi, *J. Am. Chem. Soc.*, **2012**, *134*, 9130; (c) C. Dou, S. Saito, K. Matsuo, I. Hisaki and S. Yamaguchi, *Angew. Chem. Int. Ed.*, **2012**, *51*, 12206.
- B. E. Koene, D. E. Loy and M. E. Thompson, *Chem. Mater.*, **1998**, *10*, 2235.
- M. Kranz, F. Hampel and T. Clark, *J. Chem. Soc., Chem. Commun.*, **1992**, 1247.
- Y. Kitamoto, T. Suzuki, Y. Miyata, H. Kita, K. Funaki and S. Ooi, *Chem. Commun.*, **2016**, *52*, 7098.
- (a) T. Kushida, Z. Zhou, A. Wakamiya and S. Yamaguchi, *Chem. Commun.*, **2012**, *48*, 10715; (b) H. Iwahara, T. Kushida and S. Yamaguchi, *Chem. Commun.*, **2015**, *52*, 1124; (c) N. Ando, T. Kushida and S. Yamaguchi, *Chem. Commun.*, **2018**, *54*, 5213.
- A single-point calculation of **4'** was carried out using the optimized structure of **4**, except for the alignment of the *N*-phenyl group.
- (a) P. v. R. Schleyer, C. Maerker, A. Dransfeld, H. Jiao and N. J. R. v. E. Hommes, *J. Am. Chem. Soc.*, **1996**, *118*, 6317; (b) C. Chen, C. S. Wannere, C. Corminboeuf, R. Puchta and P. v. R. Schleyer, *Chem. Rev.*, **2005**, *105*, 3842.
- (a) E. T. Seo, R. F. Nelson, J. M. Fritsch, L. S. Marcoux, D. W. Leedy and R. N. Adams, *J. Am. Chem. Soc.*, **1996**, *88*, 3498; (b) L. S. Marcoux, R. N. Adams, and S. W. Feldberg, *J. Phys. Chem.*, **1969**, *73*, 2611.